Cofactor-independent Pinacolase Directs Non-Diels-Alderase Biogenesis of the Brevianamides

Ying Ye,[1#] Lei Du,[2#] Xingwang Zhang,[3] Sean A. Newmister,[1] Wei Zhang,[3] Shuai Mu,[4] Atsushi Minami,[5] Morgan McCauley,[6] Juan V. Alegre-Requena,[7] Amy E. Fraley,[1] Maria L. Adrover-Castellano,[1] Nolan Carney,[1] Vikram V. Shende,[1] Hideaki Oikawa,[5] Hikaru Kato,[6] Sachiko Tsukamoto,[6] Robert S. Paton,[7] Robert M. Williams,[7,8*] David H. Sherman,[1,9*] and Shengying Li[2,3*]

[1]Life Sciences Institute, University of Michigan, Ann Arbor, Michigan 48109, USA

[2]Shandong Provincial Key Laboratory of Synthetic Biology, CAS Key Laboratory of Biofuels, Qingdao Institute of Bioenergy and Bioprocess Technology, Chinese Academy of Sciences, Qingdao, Shandong, 266101, China

[3]State Key Laboratory of Microbial Technology, Shandong University, Qingdao, Shandong, 266237, China

[4]Tianjin Institute of Pharmaceutical Research, Tianjin, 300193, China

[5]Department of Chemistry, Faculty of Science, Hokkaido University, Sapporo 060-0810, Japan

[6]Graduate School of Pharmaceutical Sciences, Kumamoto University, 5-1 Oe-honmachi, Kumamoto 862-0973, Japan

[7]Department of Chemistry, Colorado State University, Fort Collins, Colorado 80523, USA

[8]University of Colorado Cancer Center, Aurora, CO 80045, USA

[9]Departments of Medicinal Chemistry, Chemistry and Microbiology & Immunology, University of Michigan, Ann Arbor, MI, USA

[#]These authors contributed equally.

[*]Shengying Li: lishengying@sdu.edu.cn

[*]David H. Sherman: davidhs@umich.edu

[*]Robert M. Williams: robert.williams@colostate.edu

Abstract

Fungal bicyclo[2.2.2]diazaoctane indole alkaloids demonstrate intriguing structures and a wide spectrum of biological activities. Although biomimetic total syntheses have been completed for representative compounds of this structural family, the details of their biogenesis have remained largely uncharacterized. Among them, Brevianamide A represents the most basic form within this class bearing a dioxopiperazine core structure and a rare 3-*spiro*-ψ-indoxyl skeleton. Here, we identified the Brevianamide A biosynthetic gene cluster from *Penicillium brevicompacticum* NRRL 864 and fully elucidated the metabolic pathway by targeted gene disruption, heterologous expression, precursor incorporation studies, and *in vitro* biochemical analysis. In particular, we determined that BvnE is a cofactor-independent isomerase that is essential for selective production of Brevianamide A. Based on a high resolution crystal structure of BvnE, molecular modeling, mutational analysis, and computational studies provided new mechanistic insights into the diastereoselective formation of the 3-*spiro*-ψ-indoxyl moiety in Brevianamide A. This occurs through a biocatalyst controlled semi-Pinacol rearrangement and a subsequent spontaneous intramolecular [4+2] *hetero*-Diels-Alder cycloaddition.

Introduction

The fungal indole alkaloids bearing the unusual bicyclo[2.2.2]diazaoctane core have drawn considerable attention from natural product, synthetic and biological chemists for decades. A wealth of studies on the discovery of analogs (including semi-synthetic, synthetic and natural), biological activities and biosynthetic mechanisms have been conducted.[1] The prominent representatives of this structural class have been recognized by our and other laboratories as belonging to two main biogenetic families:[2, 3] (1) the ***dioxopiperazines*** which includes: the insecticidal Brevianamide A[4, 5] from *Penicillium brevicompactum*, the anticancer agents (-)-Notoamide A isolated from *Aspergillus protuberus* (formerly *Aspergillus* sp. MF297-2),[6, 7] and (+)-Notoamide A from *A. amoenus* (formerly *A. versicolor* NRRL 35600),[8] the anti-cancer agents Stephacidins A and B from *A. ochraceus,*[9, 10, 11, 12, 13] the Sclerotiamides,[14] the Versicolamides,[15, 16] the Taichunamides,[17, 18] the anti-fungal Waikialoids,[19] Amoenamide B,[20] the Speramides,[21, 22] and the Asperochramides;[23] and (2) the ***monooxopiperazines*** which includes: the anti-parasitic Paraherquamides from *Penicillium* spp.,[24, 25, 26, 27, 28, 29] the Asperparalines,[30, 31] the Marcfortines,[32, 33] the calmodulin-inhibiting Malbrancheamides,[34, 35, 36, 37] Chrysogenamide,[38] the Mangrovamides,[39, 40] Penioxalamine,[41] the Penicimutamides,[42, 43] and the Asperversiamides,[44] (Fig. 1). Moreover, the trend of discovering more bicyclo[2.2.2]diazaoctane indole alkaloids has not abated and it is anticipated that more congeners of the above two biogenetic families await isolation from both marine and terrestrial fungi, which will continue adding new, fascinating structural elements and biogenetic relationships to these families of alkaloids.

The first natural alkaloids comprising the bicyclo[2.2.2]diazaoctane core, were Brevianamides A and B as described by Birch and Wright in 1969, produced by *P. brevicompactum* in a ratio of ~10:1.[4] After we elucidated the correct absolute configuration of natural (+)-Brevianamide B through total synthesis,[45, 46] it became evident that the biogenesis of Brevianamides A and B must accommodate the stereochemical reality that the core tricyclic ring systems are *pseudo*-enantiomeric. Several biogenetic hypotheses based on the pioneering proposal first suggested by Porter and Sammes in 1970[47] reasoned that the bicyclo[2.2.2]diazaoctane core arises *via* an intramolecular [4+2] *hetero*-Diels-Alder (IMDA) construction (summarized in Fig. 2).[48, 49, 50, 51, 52, 53, 54] We experimentally interrogated the biogenetic proposal (illustrated in Fig. 2a), through the synthesis of ^{13}C-labeled putative Diels-Alder products (±)-**2**, but could not detect incorporation into either Brevianamide A or B in cultures of *P. brevicompactum*. Based

on these results, we then suggested the biosynthetic pathways illustrated in Fig. 2b and c. The fundamental difference between the biogenesis described in Fig. 2a, and that in Fig. 2b and c, was the sequential timing of the indole oxidation, the semi-Pinacol rearrangement and the crucial IMDA reactions. Thus, it remained conceivable that oxidation of Deoxybrevianamide E to the (*R*)-hydroxyindolenine provides species **5**, which can suffer several fates. One is N-C ring closure to co-metabolite Brevianamide E (Scheme 1); a second possibility is oxidation and tautomerization to the azadiene species **6** (Fig. 2b), which can suffer IMDA cyclization providing **3** and **4**, then undergo a final semi-Pinacol rearrangement to furnish Brevianamides A and B (*route i*). Alternatively, azadiene **6** could first suffer semi-Pinacol rearrangement to **7**, which then undergoes the IMDA construction to generate Brevianamides A and B (*route ii*).

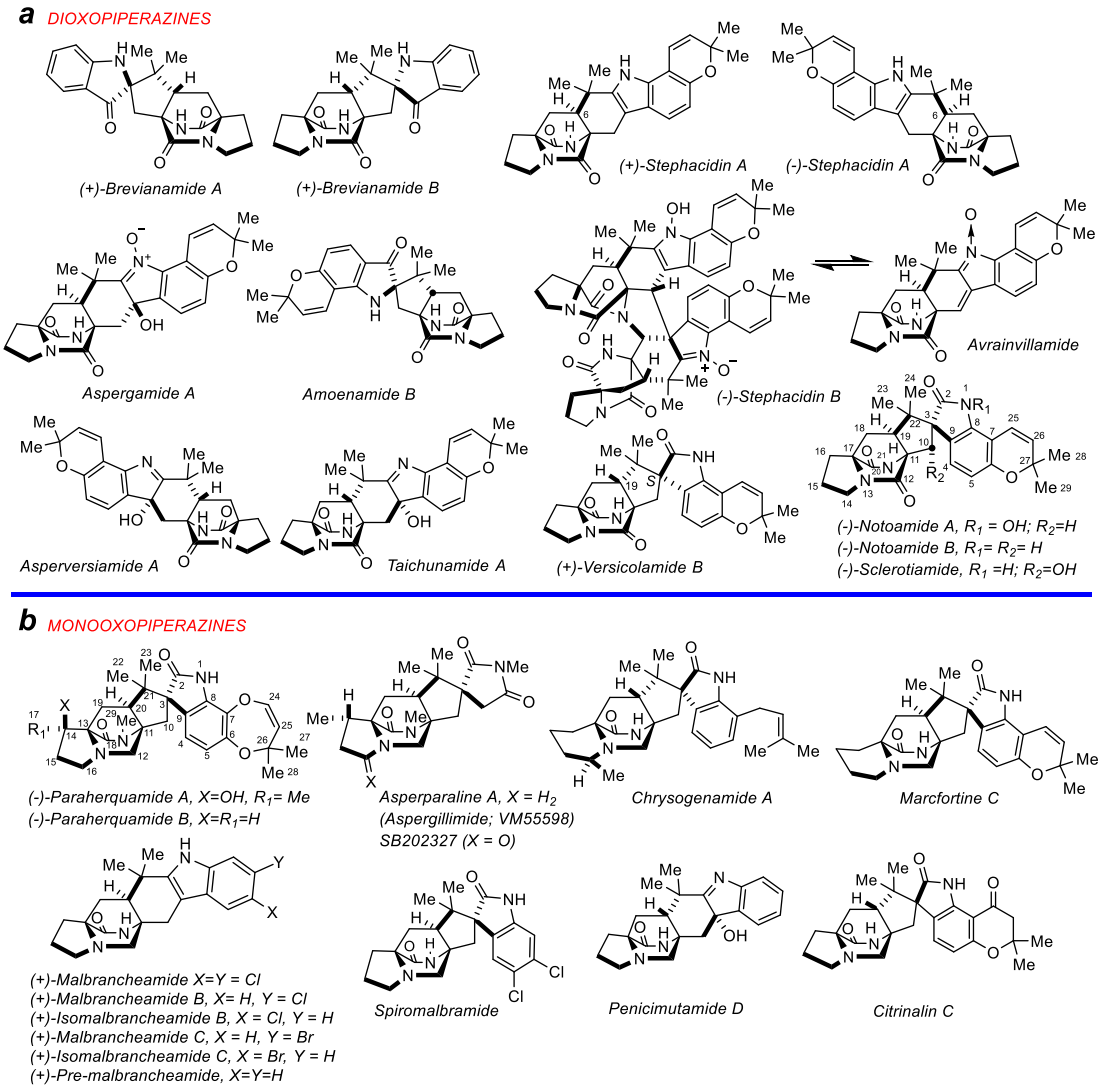

Figure 1. Representative bicyclo[2.2.2]indole alkaloids. **a.** the dioxopiperazines; **b**. the monooxopiperazines.

Another possibility (Fig. 2c) involves (*R*)-hydroxyindolenine **5**, which proceeds through a semi-Pinacol rearrangement to the indoxyl species **8**, followed by further oxidation to the azadiene species **7** and subsequent IMDA to furnish Brevianamides A and B. Experimental support to distinguish between these proposed pathways, all of which embrace the relative and absolute stereochemistry of Brevianamides A and B, have remained unresolved. However, in an attempt to generate species **7**, we found that synthetic hydroxyindolenine **10**, when treated with sodium hydroxide in DMSO-methanol, resulted in exclusive β-elimination providing the prenylated indoxyl **12** in high yield (Fig. 2d).[55] Alternatively, treatment of **10** with potassium carbonate in DMF, cleanly

furnished the oxindole species **9** in 90% isolated yield. These results initially led us to doubt the potential intermediacy of species **8**, as this compound might be anticipated to be similarly unstable to spontaneous

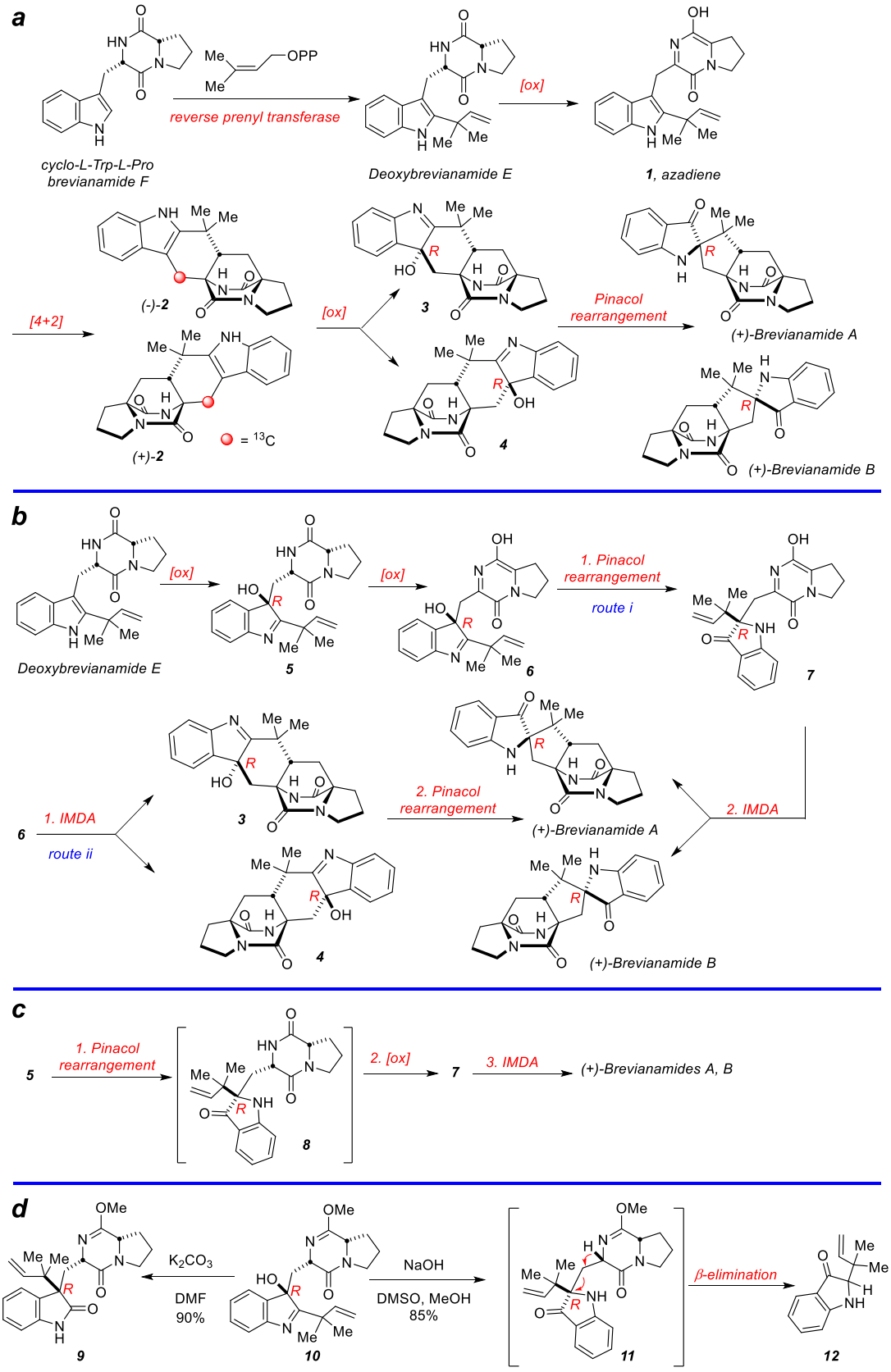

Figure 2. Biogenetic proposals for Brevianamides A and B. **a.** Early biosynthetic proposal suggested and interrogated by Williams *et al.*;[46] **b** and **c**. Original biogenesis proposed by Porter and Sammes (via **7**)[47] and more recent biosynthetic proposals suggested by Williams *et al.*;[48, 49, 54] **d.** chemical instability of non-oxidized indoxyl

11.[55]

β-elimination as observed for **10**.[55] In addition, the recent isolation of the natural hydroxyindolenines Taichunamide A,[17, 18] Asperversiamide A[44] and even Penicimutamide B,[42] provide hints that the biogenesis depicted in Fig. 2b is likely correct without being able to distinguish the two routes.

Herein, we provide new insights into the biogenesis of the Brevianamides with a focus on the indole oxidation and subsequent semi-Pinacol rearrangements. From a structural perspective, the bicyclo[2.2.2]diazaoctane metabolites are derived from highly modified, reverse-prenylated indoles, which are oxidized either before or after the critical IMDA cyclization to render ψ–indoxyls (**17**), oxindoles (**18**) or, in some instances, stable 3-hydroxyindolenines (**15**) (Fig. 3).[2, 3, 56] An important structural and biogenetic feature derives from the presumed indole 2,3-epoxidation of pathway intermediates such as Deoxybrevianamide E (Fig. 2b) or generic species **13** (Fig. 3).[57] Ring-opening of the epoxide can form a 3-hydroxyindolenine (**15**, Fig. 3), which in some instances is stable or, suffers a spontaneous semi-Pinacol rearrangement to generate 3-*spiro*-ψ-indoxyls (**17**), or *spiro*-2-oxindole species (**18**). While the *spiro*-2-oxindoles are more frequently observed in the prenylated indole alkaloid families, only a small number of 3-*spiro*-ψ-indoxyl species have been isolated, and very rarely are natural *spiro*-2-oxindole species and 3-*spiro*-ψ-indoxyls co-produced by a single microbe.[22, 58] These co-metabolite profiles strongly suggest that the semi-Pinacol rearrangement might be differentially controlled in the partitioning of the putative indole-2,3-epoxides and implies a specific biocatalyst-controlling mechanism.

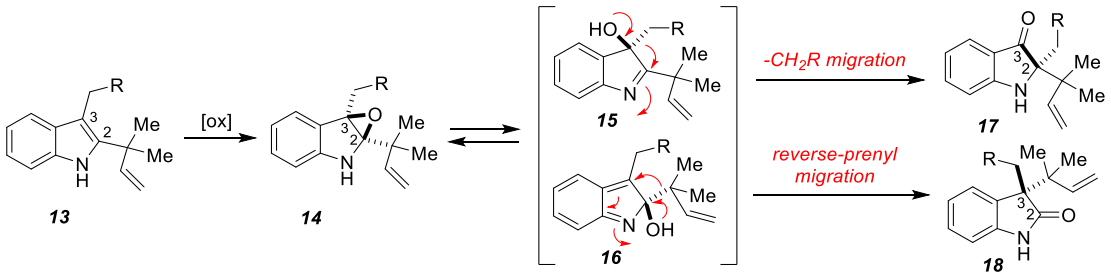

Figure 3. Disparate fates of indole-2,3-epoxide and semi-Pinacol rearrangements leading to indoxyls (**17**), oxindoles (**18**), and stable 3-hydroxyindolenines (**15**).

Pinacol or semi-Pinacol rearrangements are of great importance in the biogenesis of natural products to generate the carbonyl group through a 1,2-alkyl group shift. In addition to the indole alkaloids noted above, further examples of putative biosynthetic Pinacol rearrangements include Aflatoxin B1,[59] (+)-Asteltoxin,[60] (+)-Liphagal,[61] Tropolone,[62] and Aurachin.[63] The prevalence of this presumed transformation have motivated several studies involving semi-Pinacol rearrangements in biomimetic total syntheses (reviewed by Song *et al.*[64]). Surprisingly, natural product biosynthetic pathways that include a (semi)-Pinacol rearrangement are rare, and currently all known pinacolases are cofactor-dependent.[65] For example, the FAD-dependent monooxygenase NotB mediating biosynthesis of Notoamide C and D,[57] the non-heme iron (II) dioxygenase TropC involved in Tropolone biosynthesis,[66] and a two-enzyme system AuaG/AuaH (FAD/NADH dependent, respectively) responsible for assembly of Aurachin.[65] Each of these enzymes appears to be bifunctional; not only possessing their intrinsic oxidoreductase activity, but also directing a 1,2-alkyl shift to form the carbonyl group.

Brevianamides A and B represent the most basic structural form that contains the key functional groups

characteristic of this class of metabolites including: (1) the bicyclo[2.2.2]diazaoctane core and (2) the 3-*spiro*-ψ-indoxyl functionality. Although the chemical synthesis of Brevianamide A has recently been accomplished,[67] the various biosynthetic pathway proposals remain unresolved experimentally due to lack of access to the key enzymes. Thus, Brevianamides A and B are ideal targets for deciphering the long-standing enigma regarding the biogenesis of this important class of fungal metabolites. In this study, we identified the Brevianamide A biosynthetic gene cluster (*bvn*) and fully elucidated its metabolic pathway through complementary approaches including gene deletion in *Penicillium brevicompactum* NRRL864 (*Pb*), heterologous gene expression in *Aspergillus oryzae* NSAR1 (*Ao*), precursor feeding experiments, and *in vitro* biochemical analysis. These efforts have resulted in a biocatalytic synthesis of Brevianamides A and B in the ~10:1 ratio observed when isolated from the producing fungus (Scheme 1). This work has also enabled identification and characterization of BvnE, a novel isomerase catalyzing a semi-Pinacol rearrangement to form the 3-*spiro*-ψ-indoxyl functionality. The BvnE pinacolase is revealed to direct selectively the biosynthesis of Brevianamides A and B, and to the best of our knowledge, is the first cofactor-independent enzyme catalyzing a semi-Pinacol rearrangement.

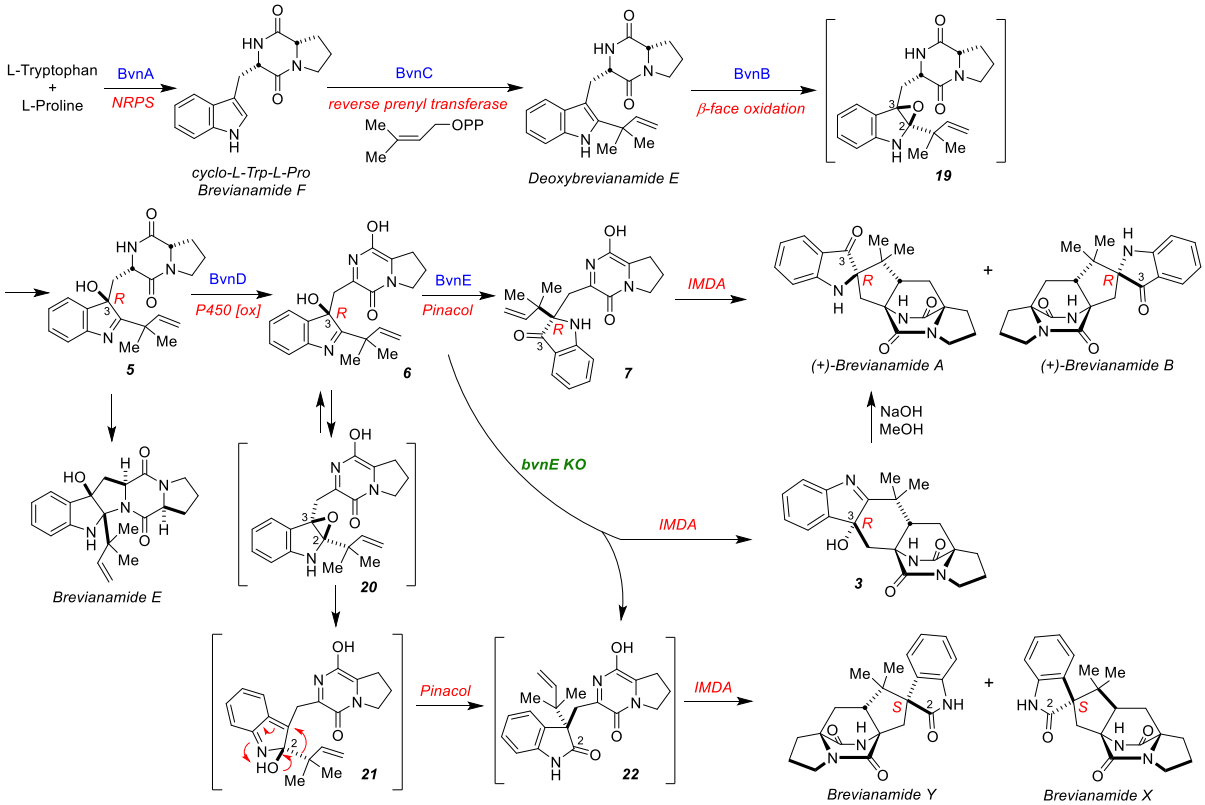

Scheme 1. Revised biosynthetic pathway for Brevianamides A and B.

Results

Brevianamide A biosynthetic gene cluster

Our long-standing interest in dissecting the biosynthetic pathways for mono- and dioxopiperazine containing indole alkaloids and the differential basis for assembly of the bicyclo[2.2.2]diazaoctane indole alkaloids[2, 3, 53, 54, 56] motivated the present study. The biosynthetic gene clusters for Brevianamide structural homologs including Notoamides, Paraherquamides and Malbrancheamides have been reported, with each comprised of a bimodular nonribosomal peptide synthetase (NPRS) responsible for the cyclodipeptide skeleton assembled from tryptophan

and proline.[2] Through genome mining using the Notoamide NRPS gene *notE* as a probe, a putative Brevianamide A biosynthetic (*bvn*) gene cluster was identified in *Pb* (Fig. 4a). The annotated *bvn* gene cluster (16 kb) is more compact than the biosynthetic gene clusters for (+)-/(-)-Notoamide A (*not/not´*, 45 kb), and reflects the relatively simple structure of Brevianamide A. The *bvn* cluster contains *bvnA* (NRPS), *bvnB* (flavin monooxygenase, FMO), *bvnC* (prenyltransferase), and *bvnD* (P450 monooxygenase, P450), all of which have close homologs (49%/64%-68%/81%, similarity/identity) compared to genes for (+)-/(-)-Notoamide A biosynthesis. Moreover, *bvnE* (465 bp) that encodes a putative isomerase shows low homology to Trt14, AusH and PrhC involved in meroterpenoid biosynthetic pathways.[68] By contrast, the biosynthetic gene clusters of the *spiro*-2-oxindole containing Notoamides, Paraherquamides, and Malbrancheamides[2] lack a *bvnE* homolog, and mining the remainder of the corresponding genomes also failed to identify a homologous gene. This finding suggested that BvnE might play an important role in formation of 3-*spiro*-ψ-indoxyl moiety.

Gene deletion in *Pb*

In the *bvn* gene cluster, the bimodular NRPS (BvnA; A-T-C-A-T-C) encoded by *bvnA* is presumed to catalyze the formation of Brevianamide F (Scheme 1). Its homologs FtmA (48%/64%, identity/similarity)[69] and NotE (49%/64%, identity/similarity)[6] were previously characterized to be responsible for generating Brevianamide F in Fumitremorgin and Notoamide biosynthesis, respectively. Here we confirmed BvnA as another Brevianamide F synthase by its heterologous expression in *Ao* (Supplementary Fig. S1). To elucidate the function of the remaining *bvnB*-*bvnE*, four individual single gene knockout (KO) strains of *Pb* were constructed. A hygromycin resistance marker was employed to replace the target gene in wild-type *Pb* (*Pb*-WT) using homologous recombination through PEG-mediated protoplast transformation (see Supplementary Methods).

Multiple protein sequence alignment (Supplementary Table S1) showed that BvnC is likely a prenyltransferase, and its homolog NotF (60%/73%, identity/similarity) was previously determined to be a Deoxybrevianamide E synthase in Notoamide biosynthesis.[6] To investigate the function of BvnC, we first deleted *bvnC* in *Pb*, and the resultant *Pb*-*bvnC*-KO strain accumulated Brevianamide F (Fig. 4b, trace ii) as the only product. The *in vitro* assay with purified recombinant BvnC showed its ability to catalyze conversion of Brevianamide F into Deoxybrevianamide E in the presence of DMAPP and Mg^{2+} (Fig. 4c, trace ii). Thus, BvnC is a Deoxybrevianamide E synthase as previously demonstrated for NotF.[6]

Next, we demonstrated that the *Pb*-*bvnB*-KO and the *Pb*-*bvnD*-KO mutant strains accumulated Deoxybrevianamide E (Scheme 1, Fig. 4b, trace iii) and Brevianamide E (Scheme 1, Fig. 4b, trace iv), respectively. Brevianamide E is proposed to be a rearranged shunt product resulting from initial 2,3-indole epoxidation of Deoxybrevianamide E by BvnB FMO. Unsurprisingly, the recombinant *N*-His_6-tagged BvnB efficiently converted Deoxybrevianamide E into Brevianamide E *in vitro* (Fig. 4d, trace ii) probably via a similar mechanism for NotB[57] (a BvnB homolog, 62%/75%, identity/similarity) in Notoamide biosynthesis. Since *Pb*-*bvnD*-KO did not produce a bicyclo[2.2.2]diazaoctane structure, we reasoned that BvnD is a key enzyme enabling production of the requisite azadiene for the proposed IMDA reaction.

Finally, when *bvnE* was deleted in *Pb*, six detectable substances were observed by HPLC in addition to low levels of Brevianamide A and B (Fig. 4b, trace v), all showing the same molecular weight of 365 Da (Supplementary Fig. S4). These include **3**, Brevianamide X, Brevianamide Y, and three unidentified isomers **UI-1**, **UI-2** and **UI-3** with the corresponding retention time of 6.3, 6.6, and 16.7 min. Instability (Supplementary Fig. S2)

prevented structural determination of these three unidentified isomers. The ratio of Brevianamide A : Brevianamide B : **3** : Brevianamide X : Brevianamide Y was determined to be 1:1:7:5:9 (Supplementary Table S2, the three unidentified isomers were not quantified due to lack of standards). The three isolable derivatives were purified and structurally determined to be a new compound **3**, and the two known metabolites Brevianamide X and Brevianamide Y[58] through high resolution mass spectrometry (HRMS) and nuclear magnetic resonance (NMR) analyses (Supplementary Table S3 and S4, Fig. S4, S17-S34). The absolute configuration of **3** was elucidated by ECD, while those of Brevianamides X and Y by single-crystal X-ray diffraction (*see below*). Brevianamide Y and **3** show the opposite stereochemistry in their bicyclo[2.2.2]diazaoctane moiety in terms of facial (*top* face *vs bottom* face) selectivity for cycloaddition (Scheme 1). Based on the spectral similarity between **3** and **UI-1** (Supplementary Fig. S5), and the observation that **UI-1** spontaneously collapsed to Brevianamide B (perhaps mimicking the spontaneous conversion of **3** to Brevianamide A) (Supplementary Fig. S11), we reason that **UI-1** is likely to be compound **4**. Since *Pb*-WT generates Brevianamide A as the dominant product compared to Brevianamide B (~10:1) (Fig. 4b, trace vi; Supplementary Table S2), we reasoned that BvnE mediates isomerization of the precursor **6** to form **7**, which is likely the direct precursor of Brevianamides A and B. In the absence of BvnE, species **6** would undergo spontaneous bond rearrangements and subsequent non-enzymatic IMDA reactions. Supporting this, the observed product profile (Fig. 4b, trace v) is quantitatively consistent with the calculated product distribution with the exception of Brevianamide X (Supplementary Table S10).

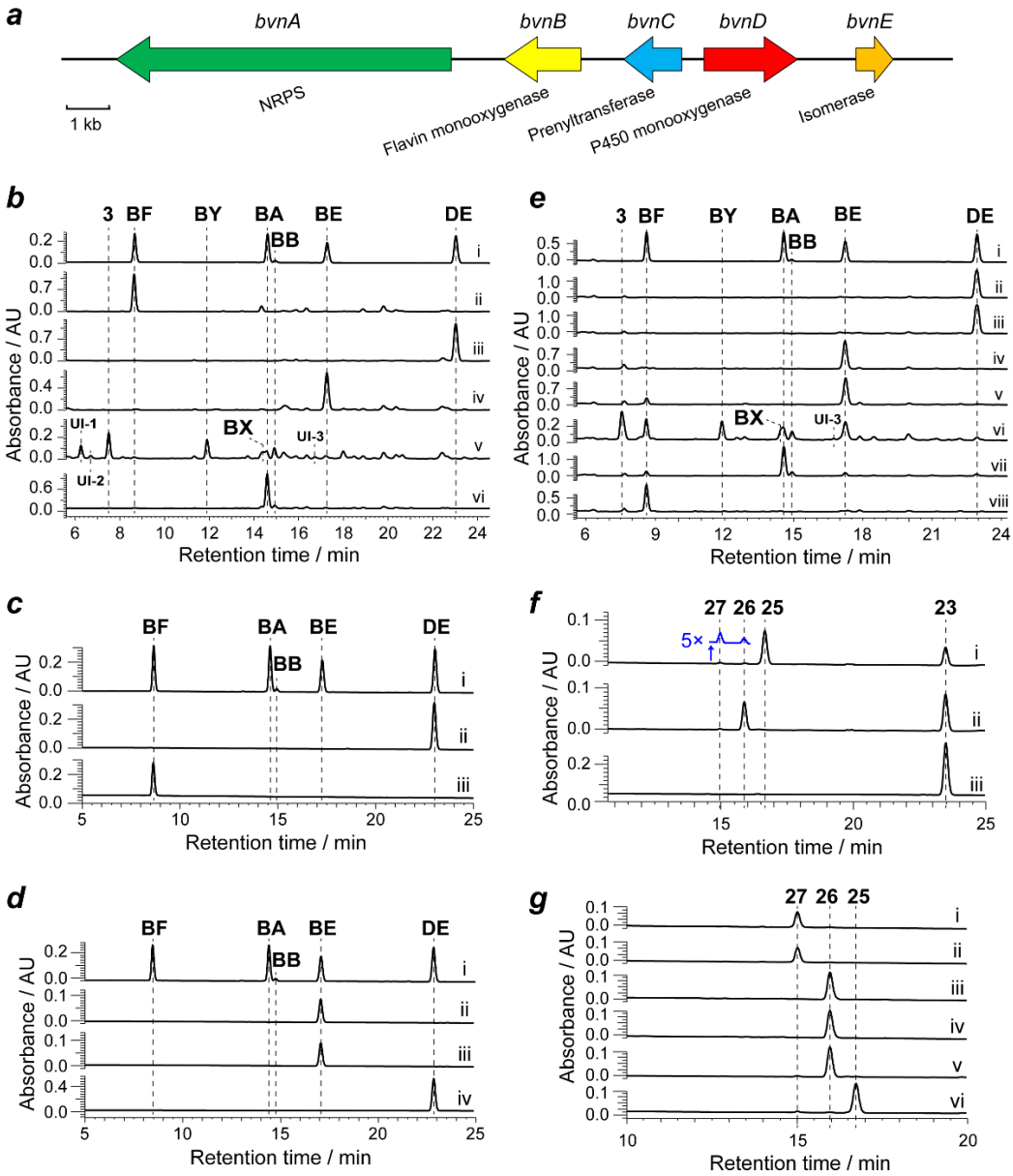

Figure 4. Overview of *bvn* gene cluster and HPLC analysis results. **a**. The *bvn* gene cluster from *Pb*; **b**–**g**. HPLC analysis (230 nm); **b**. *Pb*-WT and KO mutants. i, standards; ii-v, *Pb* KO mutants of *bvnC*, *bvnB*, *bvnD*, and *bvnE*; vi, *Pb*-WT; **c**. BvnC *in vitro* reactions. i, standards; ii, BvnC + BF; iii, boiled BvnC + BF as a control of ii; **d**. Enzymatic assays with DE as substrate. i, standards; ii, BvnB + DE; iii, BvnB + BvnE +DE; iv, boiled BvnB + DE as a control of ii; **e**, different *Ao* transformants upon feeding of BF. i, standards; ii, *Ao-bvnC*; iii, *Ao-bvnCDE*; iv, *Ao-bvnBC*; v, *Ao-bvnBCE*; vi, *Ao-bvnBCD*; vii, *Ao-bvnBCDE*; viii, *Ao*-WT; **f**. Enzymatic assays with **23** as substrate. i, BvnB + **23**; ii, BvnB + BvnE + **23**; iii, boiled BvnB + **23** as a control of ii; **g**. BvnE enzymatic assays with **25-27** as substrates. i, BvnE + **27**; ii, boiled BvnE + **27** as a control of i; iii, BvnE + **26**; iv, boiled BvnE + **26** as a control of iii; v, BvnE + **25**; vi, boiled BvnE + **25** as a control of v. BA = Brevianamide A; BB = Brevianamide B; BE = Brevianamide E; BF = Brevianamide F; BY = Brevianamide Y; DE = Deoxybrevianamide E; BX = Brevianamide X; **UI-1**, **UI-2** and **UI-3** denote the unidentified isomers.

Heterologous gene expression of *bvn* genes in *Ao*

To validate the function of *bvn* genes and also to clarify the order of biosynthetic steps, we conducted

heterologous expression with different gene combinations in *Ao*. Specifically, wild-type *Ao* (*Ao*-WT) was transformed with individual plasmids to obtain the recombinant strains for feeding of early biosynthetic intermediate Brevianamide F into growing cultures. As expected, Brevianamide F was converted into Deoxybrevianamide E by *Ao-bvnC* (Fig. 4e, trace ii). *Ao-bvnCDE* produced Deoxybrevianamide E exclusively in the feeding experiment (Fig. 4e, trace iii); *Ao-bvnBC* and *Ao-bvnBCE* both accumulated Brevianamide E exclusively (Fig. 4e, trace iv and v). These results strongly suggest that the presumed indole epoxidation catalyzed by FMO BvnB occurs *prior to* the P450 BvnD-mediated step and preceding the BvnE-catalyzed step. Upon introduction of Brevianamide F to *Ao-bvnBCD* cultures, six products (Brevianamide A, Brevianamide B, **3**, Brevianamide X, Brevianamide Y, and **UI-3**) with identical *m/z* 366 ($[M+H]^+$) were observed (Fig. 4e, trace vi; Supplementary Fig. S4) by HPLC and HRMS analysis. Their relative abundance (Brevianamide A : Brevianamide B : **3** : Brevianamide X : Brevianamide Y = 1:1:5:2:6) was roughly consistent with the observations in *Pb-bvnE*-KO (Fig. 4b, trace v; Supplementary Table S2) except that **UI-1** and **UI-2** were not detected (probably due to instability in culture conditions). Finally, when *bvnE* was incorporated, and the *Ao-bvnBCDE* strain grown in the presence of exogenous Brevianamide F, we observed Brevianamide A as the dominant product along with Brevianamide B as the minor product (~10:1 ratio) (Fig. 4e, trace vii; Supplementary Table S2).

These results demonstrated that the metabolites generated through *Ao* heterologous expression and individual *Pb bvn* deletion mutants correlated directly with one another. The reaction sequence of each enzyme in the pathway can now be deduced as BvnA→BvnC→BvnB→BvnD→BvnE. Both systems showed a BvnE-dependent change of product profile: When BvnE is present, production of Brevianamide A is increased substantially compared to Brevianamide B; When BvnE is absent, Brevianamide A and Brevianamide B are produced in almost equal levels, but much reduced compared to **3**, Brevianamide X and Brevianamide Y. Taken together, these results demonstrate that BvnE functions to catalyze formation of the 3-*spiro*-ψ-indoxyl species **7**, and directly impacts diastereocontrol of the presumed IMDA reaction.

Structure Elucidation of Brevianamide Derivatives

NMR analyses were conducted to determine the structures of Brevianamide A, **3**, Brevianamide X, and Brevianamide Y after scale-up bioconversions using the recombinant *Ao* strains. The identity of Brevianamide B was confirmed by comparisons with the corresponding chemically synthesized authentic standard regarding their HPLC retention time, co-injection experiments and HRMS (Supplementary Figs. S3 and S4). The compound with the retention time of 14.4 min and 12 min (Fig. 4b, trace v and Fig. 4e, trace vi) showed identical NMR data reported for Brevianamide X and Brevianamide Y, respectively (Supplementary Table S4 and Figs. S23-S34).[58] For the absolute configuration of these two compounds, we observed that the calculated ECD for Brevianamide X (3*S*, 11*R*, 17*R*, 19*R*) and Brevianamide Y (3*S*, 11*S*, 17*S*, 19*R*) reported by Xu *et al.*[58] cannot differentiate between these two diastereomers. To confirm the structure and absolute configuration, we conducted single-crystal X-ray diffraction analysis of both compounds (Flack parameter = 0.00(6), Fig. 5a and b and Supplementary Table S6), which confirmed their identities as Brevianamide X and Y.

Compound **3** was determined to be a new metabolite, and its molecular formula was deduced to be $C_{21}H_{23}N_3O_3$ by HRMS ($[M+H]^+$ =366.1813, Supplementary Fig. S4). The ^1H NMR spectrum of this compound (Supplementary Fig. S17) indicated that **3** is similar to Taichunamide A except for the tryptophan aromatic region. Analysis of the 2D NMR spectra (Supplementary Fig. S19-S22) was consistent with the planar structure of **3**, corresponding to

Taichunamide A without the 2,2-dimethylpyran ring. NOE correlations, H19/H_3-24, NH_{21}/H_3-23, H_{23}/OH-3 indicated the relative configurations to be 3*R**,11*R**,17*R**,19*S**. The ECD spectrum (Fig. 5c) showed a positive Cotton effect at ~ 211 nm, corresponding to the calculated 3*R* instead of 3*S* configuration. Thus, the absolute configuration of **3** was determined to be 3*R*,11*R*,17*R*,19*S*. Although produced by the same strain, compound **3** and Brevianamide Y have the *opposite* absolute stereochemistry in the bicyclo[2.2.2]diazaoctane moiety, reflecting enantio-divergent facial selectivity in the cycloaddition reaction responsible for the construction of each IMDA core (Fig. 5b and c).

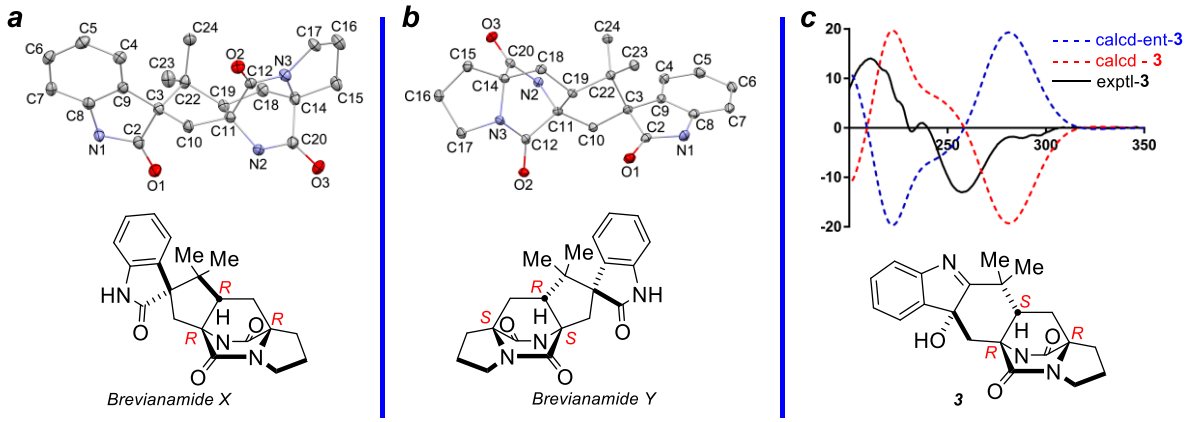

Figure 5. Structure elucidation of compound **3**, Brevianamide X and Brevianamide Y. **a.** X-ray ORTEP diagram (*top*) of brevianamide X (*bottom*); **b.** X-ray ORTEP diagram (*top*) of brevianamide Y (*bottom*); **c.** Experimental and computational ECD spectra (*top*) of **3** (*bottom*).

Functional investigation of BvnD

Having elucidated the function of BvnA, BvnC and BvnB and establishment of the reaction sequence, we next sought to characterize the following biosynthetic step presumably catalyzed by the P450 enzyme BvnD. However, intensive attempts to produce BvnD in *E. coli* and *Saccharomyces cerevisiae* were unsuccessful, thus preventing direct analysis of its functionality. Nonetheless, the results that (1) *Ao-bvnBCD* transformed Brevianamide F into multiple IMDA products including Brevianamide A, Brevianamide B, **3**, Brevianamide X and Brevianamide Y (Fig. 4e, trace vi); and (2) *Ao-bvnD* was not able to recognize Deoxybrevianamide E as a substrate (Fig. 4b, trace iii; Fig. 4e, trace iii), and the principles for P450 enzymes and DA reactions together suggest that BvnD might oxidize a non-isolable intermediate **5** (derived from ring opening of the indole epoxide **19**) to **6** in order to present the diene moiety required for IMDA cyclization (Scheme 1). In the absence of BvnD, compound **5** would collapse to Brevianamide E via an energetically favored N-C ring closure (Supplementary Figs. S55 and S56).

Although we cannot exclude the possibility that BvnD might be capable of directly desaturating the N-C bond in the dioxopiperazine ring of **5**, it is more likely that BvnD first catalyzes hydroxylation of **5** followed by spontaneous dehydration/tautomerization to yield **6**. Although multiple sites on **5** could be potentially oxidized by BvnD, all hypothetical hydroxylation products (Scheme 4; Supplementary Figs. S57) should generate the diene moiety for IMDA upon a spontaneous dehydration/tautomerization process. Bond dissociation energy (BDE) calculations (Supplementary Figs. S57) indicated that the most probable hydroxylation sites include the tertiary C-H bond at C11 or C17. We surmise that the C11 hydroxylation catalyzed by BvnD might be the most likely reaction as FtmG (a BvnD homolog with 47%/64% identity/similarity in the Fumitremorgin biosynthetic pathway)

has been experimentally confirmed to hydroxylate an analogous substrate.[70]

In vitro characterization of BvnE

Based on the results of *Pb-bvnE*-KO and *Ao-bvnBCD* (Fig. 4b and e), BvnE appeared to be a central enzyme for controlling the product profile in Brevianamide biogenesis. To assess this unique isomerase *in vitro*, the *N*-terminal His_6-tag BvnE was produced in *E. coli* BL21(DE3) and purified to homogeneity (Supplementary Fig. S6). Next, we sought to identify the potential natural substrate of BvnE from *Pb-bvnE*-KO. Compounds **3**, Brevianamides X and Y, and Brevianamide E were tested as substrates, but failed to be transformed (Supplementary Figs. S7 and S8). Thus, we hypothesized that **6** might be the substrate of BvnE. Considering the inaccessibility of this unstable intermediate, we elected to chemoenzymatically synthesize *N*-methyl-Deoxybrevianamide E (**25**) (*see* Supplementary Methods), a stable analog of **6** (Scheme 2) in order to block the dioxopiperazine nitrogen from N-C ring closure, and prevent formation of the unstable azadiene intermediate upon spontaneous dehydration. The mechanistic probe **25** was prepared through BvnB *in vitro* conversion of the chemically synthesized **23** (for HRMS and NMR analyses see Supplementary Figs. S9, S35-S42). Interestingly, two minor products **26** and **27** were also generated from **23** by BvnB along with predominant product **25** (Fig. 4g, trace i). Structural determination indicated that **26** and **27** are 3-*spiro*-ψ-indoxyl and *spiro*-2-oxindole isomers of **25**, respectively (Supplementary Table S5, Figs. S9, S43-S54). Moreover, when **25** was incubated with BvnE, it was quantitatively converted into **26** (Fig. 4g, trace v). These results revealed that BvnE is an isomerase responsible for the selective formation of the 3-*spiro*-ψ-indoxyl sub-structure (in **26**) from the 3-hydroxy-pyrrole moiety (in **25**).

Spontaneous conversion from **25** to **26** and **27** in laboratory solution conditions occurred slowly (Scheme 2; Supplementary Fig. S10). Considering the chemical similarity between **25** and **6**, one can reasonably expect that the spontaneous isomerization from **6** to **7** and **22** could also occur, which explains why multiple isomers (Brevianamides A and B, **3**, Brevianamides X and Y, and other putative diastereomers UI-1, UI-2 and UI-3 shown in Fig. 4b, trace v) were generated by the *Pb-bvnE*-KO strain.

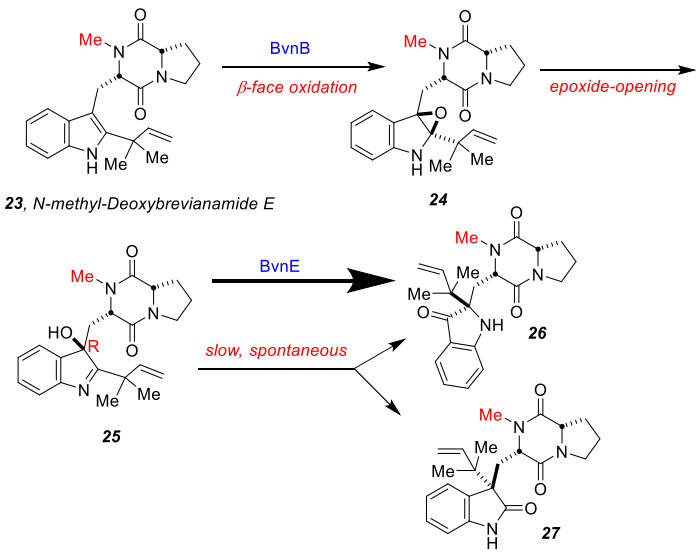

Scheme 2. BvnB and BvnE *in vitro* reactions with *N*-methylated substrates **23** and **25**.

BvnE crystal structure, docking with compound 25, and site-directed mutagenesis

BvnE belongs to a family of NTF2-like superfamily enzymes that have been previously studied in fungal meroterpenoid biogenesis.[68] As a key component in controlling product outcome in the Brevianamide biosynthesis, we sought to determine how BvnE catalyzes formation of the 3-*spiro*-ψ-indoxyl species. We solved the crystal structure of BvnE at 1.8 Å resolution (Fig. 6a) by molecular replacement using PrhC (31% sequence identity; PDB ID #: 5X9J) as a search model (final r.m.s. deviation 1.5 Å) (Supplementary Fig. S12). PrhC is a recently disclosed[68] multifunctional isomerase involved in D-ring expansion and hydrolysis during monoterpene biosynthesis in the Paraherquonin pathway.[71] PrhC and its functional homologs Trt14 and AusH display a similar overall structure to the NTF2-like superfamily enzymes,[68] despite their unique sequence and catalytic features. Similarly, BvnE is a symmetric homodimer with ~1200 $Å^2$ buried surface along the dimer interface. Each subunit shares an α+β-barrel fold composed of a six-stranded β-sheet surrounded by five α-helices. The presumed active site lies at the end of each barrel. This solvent-exposed cavity (CASTp volume 326 $Å^3$) has a predominantly hydrophobic interior and also contains several acidic and basic residues (Arg38, Tyr109, Tyr113, Glu131), which could be involved in acid-base chemistry typically reported for this family of enzymes (Fig. 6a; Supplementary Fig. S13).

Docking of the substrate **25** (Fig. 6b) and the 3-*spiro*-ψ-indoxyl product **26** (Fig. 6c) facilitated identification of the BvnE active site. Based on previous studies of BvnE structural homologs,[68] we searched for polar residues around **25**, and revealed Arg38, Tyr109, Tyr113 and Glu131 to be most likely involved in substrate binding and catalysis. These four residues were subjected to site-specific mutagenesis and *in vitro* activity assays with **25** as substrate (Scheme 2). BvnE activity in the Y109F and Y113F mutants was severely attenuated, and both E131A and E131Q mutations almost completely abolished catalysis (Fig. 6d). Additionally, BvnE variants R38A and R38Q also eliminated isomerase activity (Fig. 6d). As shown in the docking structure (Fig. 6b), Y109 and E131 are within hydrogen bonding distance from **25**, with Y109 interacting with the tryptophan carbonyl oxygen and also hydrogen bonding with Y113. Importantly, E131 has its side chain pointing toward the 3-OH of **25**, suggesting its role of hydrogen abstraction to initiate the semi-Pinacol rearrangement (Fig. 6e). Abrogation of BvnE activity by E131 mutations and the calculation results (*see below*) also supported this hypothesis. When product **26** was docked in the active site (Fig. 6c), the E131 side chain is shown to form a hydrogen bond with the proline carbonyl oxygen, and Y109 is close to the newly formed 3-oxo oxygen, which may explain the selective formation of indoxyl instead of oxindole. R38 is on the loop region around the active site and has its side chain facing the substrate, which plays an important, yet unknown role in the enzyme function. Notably, the distance between R38 and the substrate appears too far to be involved in direct interactions. On the basis of these docking studies, we propose the reaction mechanism (Fig. 6e) of BvnE includes: (1) serving as a general base to initiate the semi-Pinacol rearrangement; and (2) stabilizing the transition state through hydrogen bonding.

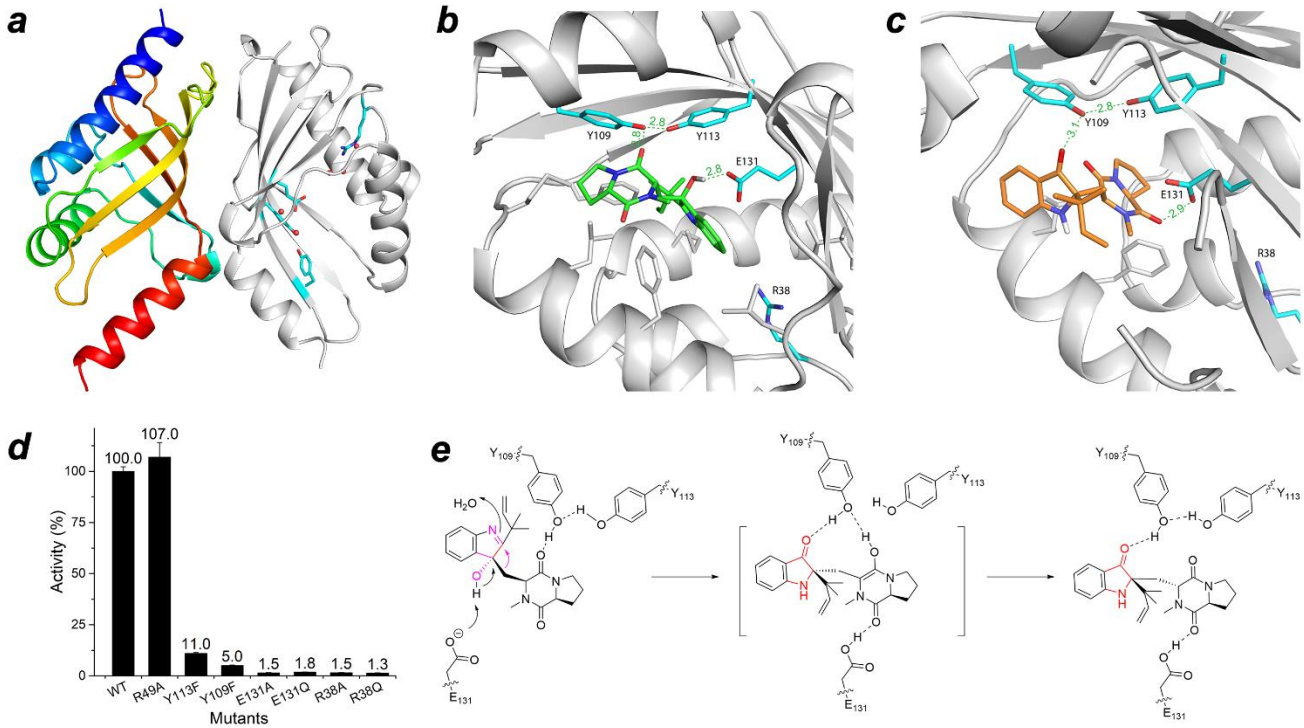

Figure 6. BvnE crystal structure, docking and the proposed reaction mechanism. **a**. Structure overview of BvnE: left chain shown in rainbow spectrum from *N*-terminus (blue) to *C*-terminus (red), the right chain in grey cartoon with putative catalytic acid-basic residues (cyan) and water molecules in active site (red spheres). **b**. BvnE-**25** (green) docking complex; **c**. BvnE-**26** (orange) complex; the mutated residues are highlighted in cyan. **d**. Site-specific mutagenesis results; **e**. Proposed BvnE reaction mechanism for isomerization of **25**.

Quantum chemical calculations

We used density functional theory calculations (DLPNO-CCSD(T)//M06-2X-D3/6-31+G(d,p))[72] to evaluate the intermediate and transition state (TS) structures in the revised biosynthetic pathway for Brevianamides A and B (Scheme 1), and to explore innate regio- and stereochemical preferences associated with key steps (Fig. 7). Accordingly, the semi-Pinacol rearrangement to form either 3-*spiro*-ψ-indoxyl **7** or *spiro*-2-oxindole **22** is favorably exergonic and irreversible (ΔG −11.6 and −24.1 kcal·mol^{-1}, respectively). Competition between these two pathways was found to be strongly dependent on whether the reaction undergoes basic activation of the hydroxyl group or acidic activation of the imine group (Fig. 7b): whereas general/specific acid activation at nitrogen results in a buildup of positive charge in the migrating group in the TS, favoring 1,2-prenyl migration (ΔΔG‡ 8.8 kcal·mol^{-1}), basic activation of the hydroxyl group has the opposite effect, inverting the selectivity to favor migration of the dioxopiperazine-containing group (ΔΔG‡ 0.7 kcal·mol^{-1}). The contrast between regioselective biosynthetic conversion of **6** into **7** and the nonselective, spontaneous conversion of **25** to **26**/**27** corroborates the involvement of E131 as a general base in BvnE (Fig. 6e) during this key step.

Distinct IMDA cyclizations were studied from intermediates **6**, **7** and **21**, **22** (Fig. 7a). In each case, there are four possible stereochemical outcomes. In this regard the levels of diastereoselectivity of IMDA of **7** are exceptional, displaying high selectivity for the formation of Brevianamide A over *pseudo*-enantantiomeric bicyclo[2.2.2]diazaoctane Brevianamide B by 2 kcal·mol^{-1}, with a very large (*ca*. 6 kcal·mol^{-1}) preference for the two *anti*-configured products over their *syn*-diastereomers. This selectivity is a result of intramolecular hydrogen

bonding in the TS structures (Fig 7a). Whereas both IMDA pathways from **6** giving rise to *anti*-configured products **3** and **4** involve a single H-bond and occur competitively, for **7** such an interaction is only present in the TS leading to major product Brevianamide A. The formation of Brevianamide Y via IMDA reactions is favored from **21** or **22,** with the pathway from **21** predicting levels of diastereoselectivity more congruent with experimental observations. All of these IMDA transformations are highly exergonic and are expected to occur irreversibly: the activation barriers are consistent with room-temperature reactivity over the course of minutes/hours. The stereospecific conversion of **3** into Brevianamide A, via a ring-contraction was found to be more challenging than the earlier 1,2-rearrangements (higher activation barrier by 11 kcal·mol^{-1}), however, this is exergonic by 4 kcal·mol^{-1}. This ring-contraction can be accomplished under laboratory conditions by treating **3** with sodium hydroxide in water (Scheme 1).

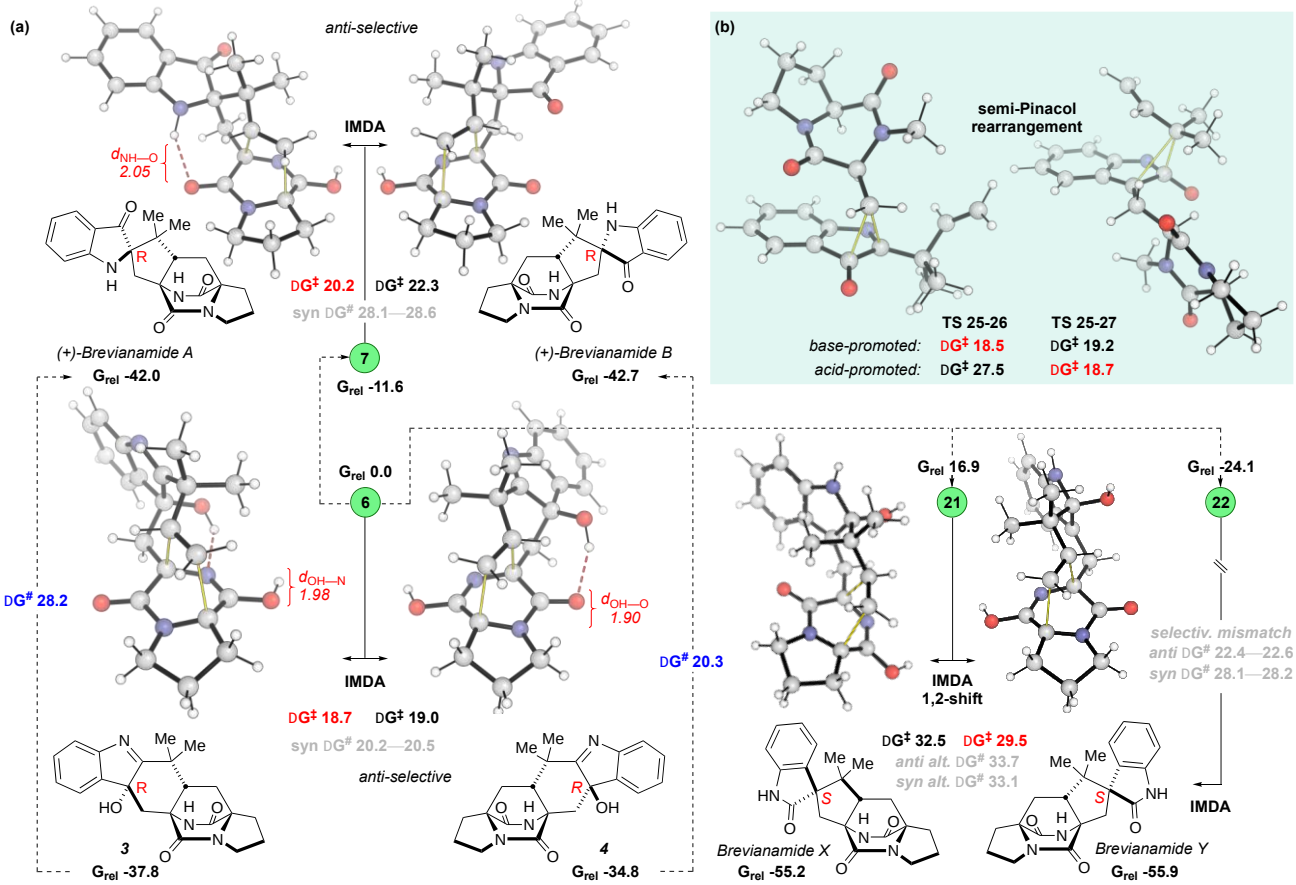

Figure 7. a. *anti*-Selective IMDA transition structures and products accessible from intermediates **6**, **7**, **21**, and **22**; **b.** 1,2-alkyl shift (semi-Pinacol) transition structures for the migration of CH_2-diketopiperazine (LHS) and reverse-prenyl (RHS) groups. Computed Gibbs energies are in kcal/mol and highlighted distances in Å.

Discussion

Pericyclic reactions in natural product biosynthesis have been recognized across numerous structural classes and include inter- and intramolecular Diels-Alder reactions mediated by a range of fascinating enzymes.[73, 74] The fungal indole alkaloids bearing the bicyclo[2.2.2]diazaoctane core have evolved two distinct pathways for the biogenesis of the monooxopiperazine and dioxopiperazine families. Moreover, we have established that two distinct branch points involving the order of Diels-Alder reaction or semi-Pinacol rearrangement are apparent in these systems. Due to challenges involving soluble expression of fungal P450s, we employed gene disruption,

heterologous gene expression, precursor feeding, and *in vitro* biochemical assays to dissect Brevianamide assembly in this study, which resolves a biosynthetic proposal first described by Birch in 1969[4] and Sammes in 1970.[47]

Our findings reveal a new order of IMDA cyclization that constructs the core bicyclo[2.2.2]diazaoctane ring system and indole 2,3-oxidation in Brevianamide biosynthesis. The well-characterized dioxopiperazine compounds such as the Notoamides, and monooxopiperazine compounds such as the Paraherquamides, are all fashioned in a biosynthetic sequence involving elaboration of a bicyclo[2.2.2]diazaoctane ring system first, followed by FMO-catalyzed indole 2,3-oxidation and semi-Pinacol rearrangement to render the 2-*spiro*-oxindoles.[2] However, for the Brevianamides, this sequence is reversed, and is reminiscent of the production of shunt products Notoamides C and D in the Notoamide pathway.[57] However, compared to Notoamide C, which is apparently not further metabolized, the P450 enzyme BvnD in the Brevianamide pathway directs the oxidized indole intermediate **5** to suffer subsequent oxidation to an azadiene species, which then undergoes the IMDA cyclization. Our elucidation of this unprecedented biogenetic sequence reflects the plasticity of diversified biosynthetic strategies that these genetically related fungi deploy for creating structurally diverse *spiro*-cyclized indole alkaloids.

Here we achieved the first total biocatalytic synthesis of the Brevianamides in *Ao* heterologous hosts, and constructed the complex chemical structure of the bicyclo[2.2.2]diazaoctane core by expressing the BvnD P450 enzyme. IMDA products require the two-electron oxidation by BvnD to provide the azadiene group, however, in the Brevianamide pathway, the [4+2] IMDA is likely a spontaneous process that follows the formation of **6**, **7** and **22** (Scheme 1) rather than an enzymatic reaction catalyzed by BvnD. This conclusion is based on (1) laboratory corroboration that ambient temperature cycloadditions from authentic azadiene species **22** has been accomplished (Scheme 3); and (2) it is difficult to imagine that a Diels-Alderase can accommodate several distinct substrates in a common active site for diastereo-divergent cyclization, leading to the experimentally observed Brevianamides A and B, **3**, Brevianamides X and Y, and other diastereomeric products (Fig. 4b trace v and 4e trace vi) in both *Pb-bvnE*-KO and Brevianamide F-fed *Ao-bvnBCD*. Nonetheless, understanding the precise functionality of BvnD through *in vitro* biochemical studies remains a high priority objective.

Furthermore, we predicted in 2003,[54] that hydroxyindolenine **5** could reasonably suffer oxidation to the azadiene species **6** *prior to* the semi-Pinacol rearrangement; IMDA cyclization would then furnish the hydroxyindolenines **3** and **4** (Fig. 2) leading to Brevianamides A and B through a final semi-Pinacol rearrangement. This prediction has now been realized by the *bvnE* knockout experiments (Scheme 1) where hydroxyindolenine **3** is indeed produced, and **4** (likely to be **UI-1**) also appears to be produced (Fig. 4). It is also significant to note that hydroxyindolenine **3** is not converted to Brevianamide A upon exposure to BvnE, further indicating that this pinacolase operates on oxidized piperazinedione substrates *before* the IMDA construction. Compound **3** does however, rearrange to Brevianamide A spontaneously in DMSO or more rapidly when treated with base (Supplementary Fig. S11).

We also synthesized Brevianamide Y by the biomimetic route shown below (Scheme 3; Supplementary Methods) wherein optically pure β-hydroxyproline-derived species **33** was subjected to *spiro*-oxindole formation by *t*-butyl hypochlorite oxidation and Pinacol rearrangement to give a diastereomeric mixture of **34**. Mitsunobu dehydration furnished the unsaturated species **35** that was subjected to treatment with KOH in methanol to give Brevianamide Y. The synthetic material matched the data reported for Brevianamide Y. As expected, the *anti*-diastereomer (Brevianamide Y) was the major product as supported by theoretical calculations (Fig. 7), in which *anti*-configuration products are favored by several kcal·mol^{-1} and Brevianamide Y is favored modestly over

the *pseudo*-enantiomeric bicyclo[2.2.2]diazaoctane. Moreover, several aspects are noteworthy here: First, the oxindole species **35** is a stable compound and does not suffer fragmentation as discussed above for a related indoxyl substrate **11** (Fig. 2). Secondly, we have generated proposed biosynthetic intermediate **22** (Scheme 1), which validates that Brevianamide Y does not require a specific Diels-Alderase for mediating the conversion of **6** to Brevianamide Y as this cycloaddition occurs at room temperature in aqueous methanolic KOH. The same is likely true for azadiene **7** that, once generated from the BvnD and BvnE sequence from **5**, will spontaneously undergo IMDA cyclization to generate Brevianamides A and B without the need for a Diels-Alderase.

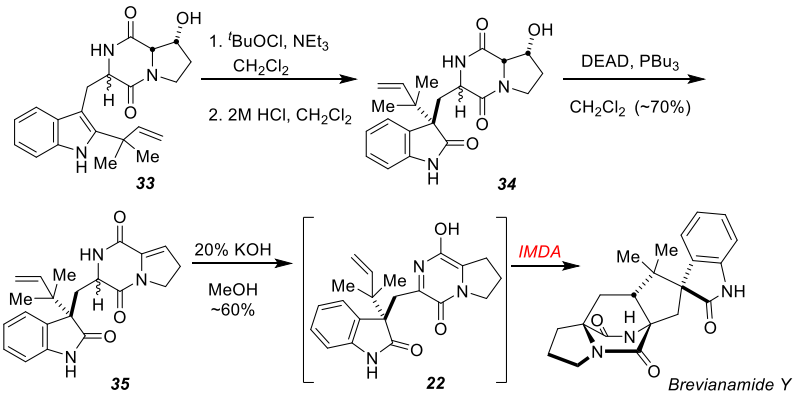

Scheme 3. Biomimetic synthesis of Brevianamide Y.

Regarding the exact reaction catalyzed by BvnD, oxidation of **5** to the azadiene species could occur via many plausible intermediates. As shown in Scheme 4, reasonable oxidation intermediates include: the *N*-hydroxylated species **28**; the two α-C-hydroxylated species **29** and **30**; and the two desaturated alkenes **31** and **32**. Precedent for each mode of hydroxylation exists based on metabolite profiles in alkaloids isolated from fungi. For example, Notoamide M[15] contains the α-C-hydroxylated proline species similar to **30**. Dehydronotoamide C with an unsaturated proline moiety similar to **31** was reported from an *Aspergillus* sp. recently.[75] *N*-hydroxylated piperazinediones are also well-known fungal metabolites.[76] We currently do not know the precise structure of the species generated from **5** by BvnD on the way to the azadiene species **6** and this constitutes a current focus of our investigations. Nonetheless, any of the species **28-32** depicted in Scheme 4 represent the oxidation state of the azadiene and can reasonably dehydrate and tautomerize to azadiene **6**. Indeed, we have validated tautomerizations of desaturated species corresponding to **31** and **32** to the corresponding azadienes in biomimetic total syntheses of the Brevianamides, Stephacidins, Notoamides and other natural members of this family in the laboratory.[56]

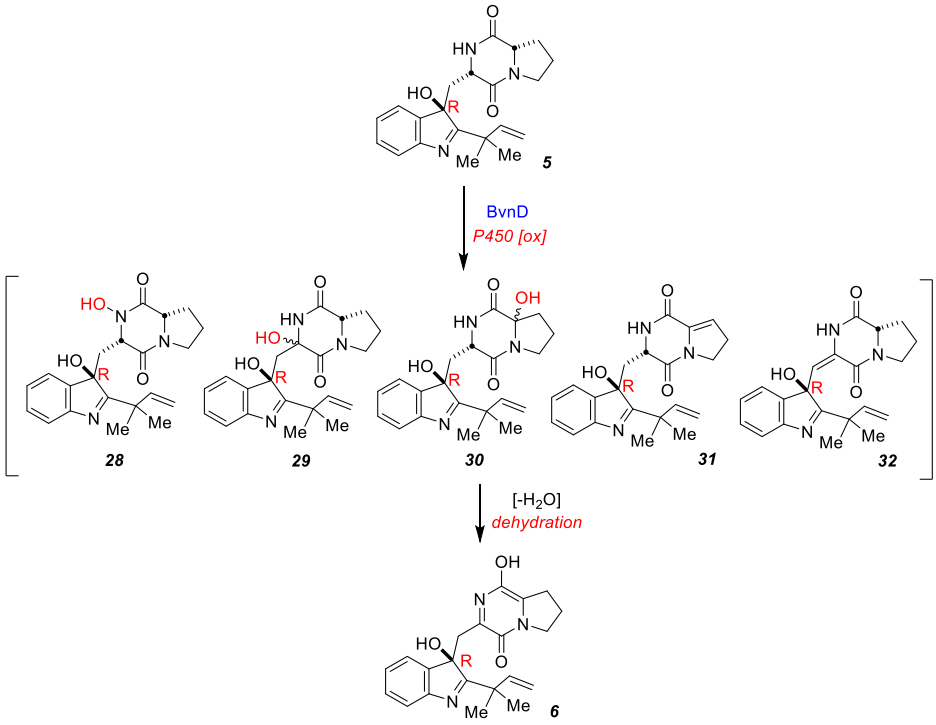

Scheme 4. Possible structures of BvnD oxidation intermediate progenitors to the azadiene.

The discovery of BvnE as a key component for control of the Brevianamide pathway product profile reveals the unique role of this small protein. It is also the first time that this type of enzyme has been shown to function in assembly of fungal *spiro*-indole alkaloids. BvnE employs acid-base chemistry to guide the direction of the Brevianamide pathway, and is an indispensable component for efficient and selective production of Brevianamides A and B. Although we have thus far been unable to isolate the native substrate of BvnE (likely unstable due to spontaneous IMDA cyclization), we synthesized **25** and with this probe were able to characterize the activity of BvnE *in vitro*, demonstrating that it directs the semi-Pinacol rearrangement toward 3-oxo indoxyl formation, which is consistent with *in vivo* genetics (*Pb-bvnE*-KO). The BvnE crystal structure, and docking of **25** enabled us to delineate a catalytic mechanism supported by mutational analysis (Fig. 6). Thus, BvnE was revealed to be a novel enzyme catalyzing the semi-Pinacol rearrangement in a cofactor-independent manner. It is now clear that BvnE directs the Brevianamide pathway through the **6→7** transformation, leading to the generation of the 3-*spiro*-ψ-indoxyl species (Scheme 1). Production of Brevianamides A and B in a ratio of ~10:1 (Fig. 4b and c) in the presence of BvnE is likely the manifestation of thermodynamic control (Fig. 7).

In conclusion, we have characterized and fully reconstituted Brevianamides A and B biosynthesis, and identified an isomerase/Pinacolase BvnE as a key enzyme for biocatalytic control of the pathway. BvnE was characterized biochemically and structurally to be the first cofactor-free enzyme for catalyzing the semi-Pinacol rearrangement. The [4+2] IMDA-derived dioxopiperazine bicyclo[2.2.2]diazaoctane core construction has also been demonstrated for the first time and the data support a spontaneous pericyclic reaction. Several fascinating mechanistic questions nonetheless remain, including: (1) what are the mechanistic details of the BvnD-catalyzed two-electron oxidation required for azadiene formation to enable the IMDA construction?; and (2) what, if any, biogenetic relationships exist between Brevianamide biogenesis and that of other dioxopiperazine families constituted of the bicyclo[2.2.2]diazaoctane ring system, such as Notoamide A? Efforts are currently underway in

our laboratories to resolve these intriguing biosynthetic questions.

Acknowledgements

This work was supported by the National Natural Science Foundation of China (21472204 to S.L. and 31800041 to L.D.), the National Institutes of Health R01 CA070375 (to R.M.W. and D.H.S.), R35 GM118101, the Hans W. Vahlteich Professorship (to D.H.S.), the Shandong Provincial Natural Science Foundation (ZR2017ZB0207 to W.Z. and S.L. and ZR201807060986 to L.D.), the National Postdoctoral Innovative Talents Support Program (BX20180325 to L.D.), China Postdoctoral Science Foundation (2019M652500 to L.D.), and funding from NSF grant CHE-0840456 (for X-ray instrumentation). GM/CA@APS is supported by the National Institutes of Health, National Institute of General Medical Sciences (AGM-12006) and National Cancer Institute (ACB-12002). We also thank Professor Janet L. Smith from University of Michigan for her assistance with the structure determination of BvnE.

Author Contributions Y.Y., L.D., D.H.S., S.L. contributed to the experimental design. Y.Y., L.D. and W.Z. performed molecular cloning, fungal genetics and compounds purification. Y.Y., L.D. and X.Z. performed structural assignment (NMR analysis). Y.Y., L.D., S.A.N., A.E.F. and M.L.A. performed molecular cloning, protein expression and purification. Y.Y., L.D. performed enzymatic assays and LC/MS and HPLC analysis. S.A.N. and M.L.A. carried out all crystallographic experiments, structural analysis. Y.Y. performed structure-based site-directed mutagenesis. W.Z performed genome mining of the gene cluster. M.M., N.C., V.V.S. and S.M. synthesized and validated the compounds described in this study. J.V.A. and R.S.P. performed DFT calculations. A.M. and H.O. supplied the heterologous expression system. H.K. and S.T. performed ECD measurement and calculations. Y.Y., L.D., S.A.N., R.S.P., R.M.W., D.H.S. and S.L. analyzed the data and prepared the manuscript.

References

1. Klas KR, Kato H, Frisvad JC, Yu F, Newmister SA, Fraley AE*, et al.* Structural and stereochemical diversity in prenylated indole alkaloids containing the bicyclo[2.2.2]diazaoctane ring system from marine and terrestrial fungi. *Nat Prod Rep* 2018, **35**(6)**:** 532-558.

2. Li S, Srinivasan K, Hong T, Yu F, Finefield JM, Sunderhaus JD*, et al.* Comparative analysis of the biosynthetic systems for fungal bicyclo 2.2.2 diazaoctane indole alkaloids: the (+)/(-)-notoamide, paraherquamide and malbrancheamide pathways. *MedChemComm* 2012, **3**(8)**:** 987-996.

3. Finefield JM, Frisvad JC, Sherman DH, Williams RM. Fungal origins of the bicyclo 2.2.2 diazaoctane ring system of prenylated indole alkaloids. *J Nat Prod* 2012, **75**(4)**:** 812-833.

4. Birch AJ, Wright JJ. The brevianamides: a new class of fungal alkaloid. *J Chem Soc D* 1969(12)**:** 644b-645.

5. Paterson RRM, Simmonds MJS, Kemmelmeier C, Blaney WM. Effects of brevianamide A, its photolysis product brevianamide D, and ochratoxin A from two *Penicillium* strains on the insect pests *Spodoptera frugiperda* and *Heliothis virescens*. *Mycol Res* 1990, **94:** 538-542.

6. Ding Y, de Wet JR, Cavalcoli J, Li S, Greshock TJ, Miller KA*, et al.* Genome-based characterization of two prenylation steps in the assembly of the stephacidin and notoamide anticancer agents in a marine-derived *Aspergillus* sp. *J Am Chem Soc* 2010, **132**(36)**:** 12733-12740.

7. Kato H, Yoshida T, Tokue T, Nojiri Y, Hirota H, Ohta T*, et al.* Notoamides A-D: prenylated indole alkaloids isolated from a marine-derived fungus, *Aspergillus* sp. *Angew Chem Int Ed* 2007, **46**(13)**:** 2254-2256.

8. Greshock TJ, Grubbs AW, Jiao P, Wicklow DT, Gloer JB, Williams RM. Isolation, structure elucidation, and biomimetic total synthesis of versicolamide B, and the isolation of antipodal (-)-stephacidin A and (+)-notoamide B from *Aspergillus versicolor* NRRL 35600. *Angew Chem Int Ed* 2008, **47**(19)**:** 3573-3577.

9. Qian-Cutrone JF, Huang S, Shu YZ, Vyas D, Fairchild C, Menendez A*, et al.* Stephacidin A and B: two structurally novel, selective inhibitors of the testosterone-dependent prostate LNCaP cells. *J Am Chem Soc* 2002, **124**(49)**:** 14556-14557.

10. von Nussbaum F. Stephacidin B - A new stage of complexity within prenylated indole alkaloids from fungi. *Angew Chem Int Ed* 2003, **42**(27)**:** 3068-3071.

11. Fenical W, Jensen PR, Cheng XC, inventors; University of California, San Diego, San Diego, CA, USA, assignee. Avrainvillamide, a cytotoxic marine natural product, and derivatives thereof patent US 6066635. 2000 May 23, 2000.

12. Sugie Y, Hirai H, Inagaki T, Ishiguro M, Kim YJ, Kojima Y*, et al.* A new antibiotic CJ-17,665 from *Aspergillus ochraceus*. *J Antibiot* 2001, **54**(11)**:** 911-916.

13. Kito K, Ookura R, Kusumi T, Namikoshi M, Ooi T. X-ray structures of two stephacidins, heptacyclic alkaloids from the marine-derived fungus *Aspergillus ostianus*. *Heterocycles* 2009, **78**(8)**:** 2101-2106.

14. Whyte AC, Gloer JB, Wicklow DT, Dowd PF. Sclerotiamide: a new member of the paraherquamide class with potent antiinsectan activity from the sclerotia of *Aspergillus sclerotiorum*. *J Nat Prod* 1996, **59**(11)**:** 1093-1095.

15. Tsukamoto S, Kawabata T, Kato H, Greshock TJ, Hirota H, Ohta T*, et al.* Isolation of antipodal (-)-versicolamide B and notoamides L-N from a marine-derived *Aspergillus* sp. *Org Lett* 2009, **11**(6)**:** 1297-1300.

16. Liu L, Wang L, Bao L, Ren J, Basnet BB, Liu R*, et al.* Versicoamides F-H, Prenylated lndole Alkaloids from Aspergillus tennesseensis. *Org Lett* 2017, **19**(4)**:** 942-945.

17. Miller KA, Tsukamoto S, Williams RM. Asymmetric total syntheses of (+)- and (-)-versicolamide B and

biosynthetic implications. *Nat Chem* 2009, **1**(1)**:** 63-68.

18. Li F, Zhang Z, Zhang G, Che Q, Zhu T, Gu Q*, et al.* Determination of taichunamide H and structural revision of taichunamide A. *Org Lett* 2018, **20**(4)**:** 1138-1141.

19. Wang X, You J, King JB, Powell DR, Cichewicz RH. Waikialoid a suppresses hyphal morphogenesis and inhibits biofilm development in pathogenic *Candida albicans*. *J Nat Prod* 2012, **75**(4)**:** 707-715.

20. Sugimoto K, Sadahiro Y, Kagiyama I, Kato H, Sherman DH, Williams RM*, et al.* Isolation of amoenamide A and five antipodal prenylated alkaloids from *Aspergillus amoenus* NRRL 35600. *Tetrahedron Lett* 2017, **58**(29)**:** 2797-2800.

21. Chang Y-W, Yuan C-M, Zhang J, Liu S, Cao P, Hua H-M*, et al.* Speramides A-B, two new prenylated indole alkaloids from the freshwater-derived fungus *Aspergillus ochraceus* KM007. *Tetrahedron Lett* 2016, **57**(45)**:** 4952-4955.

22. Kai A, Kato H, Sherman DH, Williams RM, Tsukamoto S. Isolation of a new indoxyl alkaloid, Amoenamide B, from *Aspergillus amoenus* NRRL 35600: biosynthetic implications and correction of the structure of Speramide B. *Tetrahedron Lett* 2018, **59**(48)**:** 4236-4240.

23. Wen H, Liu X, Zhang Q, Deng Y, Zang Y, Wang J*, et al.* Three new indole diketopiperazine alkaloids from *Aspergillus ochraceus*. *Chem Biodivers* 2018, **15**(4).

24. Yamazaki M, Fujimoto H, Okuyama E, Ohta Y. On the structure of two new metabolites isolated from *Penicillium paraherquei* and *Aspergillus silvaticus*. *Proc Jpn Assoc Mycotoxicol* 1980, **10:** 27-28.

25. Yamazaki M, Okuyama E, Kobayashi M, Inoue H. The structure of paraherquamide, a toxic metabolite from *Penicillium paraherquei*. *Tetrahedron Lett* 1981, **22**(2)**:** 135-136.

26. Blanchflower SE, Banks RM, Everett JR, Manger BR, Reading C. New paraherquamide antibiotics with anthelmintic activity. *J Antibiot* 1991, **44**(5)**:** 492-497.

27. Blanchflower SE, Banks RM, Everett JR, Reading C. Further novel metabolites of the paraherquamide family. *J Antibiot* 1993, **46**(9)**:** 1355-1363.

28. Liesch JM, Wichmann CF. Novel antinematodal and antiparasitic agents from *Penicillium charlesii*. II. Structure determination of paraherquamides B, C, D, E, F, and G. *J Antibiot* 1990, **43**(11)**:** 1380-1386.

29. Kwon J, Seo YH, Lee J-E, Seo E-K, Li S, Guo Y*, et al.* Spiroindole alkaloids and spiroditerpenoids from *Aspergillus duricaulis* and their potential neuroprotective effects. *J Nat Prod* 2015, **78**(11)**:** 2572-2579.

30. Hayashi H, Nishimoto Y, Nozaki H. Asperparaline A, a new paralytic alkaloid from *Aspergillus japonicus* JV-23. *Tetrahedron Lett* 1997, **38**(32)**:** 5655-5658.

31. Banks RM, Blanchflower SE, Everett JR, Manger BR, Reading C. Novel anthelmintic metabolites from an *Aspergillus* species; the aspergillimides. *J Antibiot* 1997, **50**(10)**:** 840-846.

32. Polonsky J, Merrien MA, Prange T, Pascard C, Moreau S. Isolation and structure (X-ray analysis) of marcfortine A, a new alkaloid from *Penicillium roqueforti*. *J Chem Soc D* 1980(13)**:** 601-602.

33. Prange T, Billion MA, Vuilhorgne M, Pascard C, Polonsky J, Moreau S. Structures of marcfortine B and C (X-ray analysis), alkaloids from *Penicillium roqueforti*. *Tetrahedron Lett* 1981, **22**(21)**:** 1977-1980.

34. Beyett TS, Fraley AE, Labudde E, Patra D, Coleman RC, Eguchi A*, et al.* Perturbation of the interactions of calmodulin with GRK5 using a natural product chemical probe. *Proc Natl Acad Sci U S A* 2019.

35. Figueroa M, Gonzalez MDC, Mata R. Malbrancheamide B, a novel compound from the fungus *Malbranchea aurantialca*. *Nat Prod Res* 2008, **22**(8)**:** 709-714.

36. Martinez-Luis S, Rodriguez R, Acevedo L, Gonzalez MC, Lira-Rocha A, Mata R. Malbrancheamide, a new calmodulin inhibitor from the fungus *Malbranchea aurantiaca*. *Tetrahedron* 2006, **62**(8)**:** 1817-1822.

37. Watts KR, Loveridge ST, Tenney K, Media J, Valeriote FA, Crews P. Utilizing DART mass spectrometry to pinpoint halogenated metabolites from a marine invertebrate-derived fungus. *J Org Chem* 2011, **76**(15)**:** 6201-6208.

38. Lin Z, Wen J, Zhu T, Fang Y, Gu Q, Zhu W. Chrysogenamide a from an endophytic fungus associated with *Cistanche deserticola* and its neuroprotective effect on SH-SY5Y cells. *J Antibiot* 2008, **61**(2)**:** 81-85.

39. Yang B, Dong J, Lin X, Zhou X, Zhang Y, Liu Y. New prenylated indole alkaloids from fungus *Penicillium* sp derived of mangrove soil sample. *Tetrahedron* 2014, **70**(25)**:** 3859-3863.

40. Yang B, Tao H, Lin X, Wang J, Liao S, Dong J*, et al.* Prenylated indole alkaloids and chromone derivatives from the fungus *Penicillium* sp SCSI0041218. *Tetrahedron* 2018, **74**(1)**:** 77-82.

41. Hu X-L, Bian X-Q, Wu X, Li J-Y, Hua H-M, Pei Y-H*, et al.* Penioxalamine A, a novel prenylated spiro-oxindole alkaloid from *Penicillium oxalicum* TW01-1. *Tetrahedron Lett* 2014, **55**(29)**:** 3864-3867.

42. Li C-W, Wu C-J, Cui C-B, Xu L-L, Cao F, Zhu H-J. Penicimutamides A-C: rare carbamate-containing alkaloids from a mutant of the marine-derived *Penicillium purpurogenum* G59. *Rsc Advances* 2016, **6**(77)**:** 73383-73387.

43. Wu C-J, Li C-W, Gao H, Huang X-J, Cui C-B. Penicimutamides D-E: two new prenylated indole alkaloids from a mutant of the marine-derived *Penicillium purpurogenum* G59. *Rsc Advances* 2017, **7**(40)**:** 24718-24722.

44. Li H, Sun W, Deng M, Zhou Q, Wang J, Liu J*, et al.* Asperversiamides, linearly fused prenylated indole alkaloids from the marine-derived fungus *Aspergillus versicolor*. *J Org Chem* 2018, **83**(15)**:** 8483-8492.

45. Williams RM, Glinka T, Kwast E. Facial selectivity of the intramolecular SN2' cyclization: stereocontrolled total synthesis of brevianamide B. *J Am Chem Soc* 1988, **110**(17)**:** 5927-5929.

46. Williams RM, Kwast E, Coffman H, Glinka T. Remarkable, enantio-divergent biogenesis of brevianamide A and B. *J Am Chem Soc* 1989, **111**(8)**:** 3064-3065.

47. Porter AEA, Sammes PG. A Diels-Alder reaction of possible biosynthetic importance. *J Chem Soc D* 1970(17)**:** 1103a.

48. Sanzcervera JF, Glinka T, Williams RM. Biosynthesis of the brevianamides: quest for a biosynthetic Diels-Alder cyclization. *J Am Chem Soc* 1993, **115**(1)**:** 347-348.

49. Sanzcervera JF, Glinka T, Williams RM. Biosynthesis of brevianamides A and B: in search of the biosynthetic Diels-Alder construction. *Tetrahedron* 1993, **49**(38)**:** 8471-8482.

50. Williams RM, Sanz-Cervera JF, Sancenon F, Marco JA, Halligan K. Biomimetic Diels-Alder cyclizations for the construction of the brevianamide, paraherquamide sclerotamide, and VM55599 ring systems. *J Am Chem Soc* 1998, **120**(5)**:** 1090-1091.

51. Williams RM, Sanz-Cervera JF, Sancenon F, Marco JA, Halligan KM. Biomimetic Diels-Alder cyclizations for the construction of the brevianamide, paraherquamide, sclerotamide, asperparaline and VM55599 ring systems. *Biorg Med Chem* 1998, **6**(8)**:** 1233-1241.

52. Adams LA, Valente MWN, Williams RM. A concise synthesis of d,l-brevianamide B via a biomimetically-inspired IMDA construction. *Tetrahedron* 2006, **62**(22)**:** 5195-5200.

53. Williams RM, Cox RJ. Paraherquamides, brevianamides, and asperparalines: laboratory synthesis and biosynthesis. An interim report. *Acc Chem Res* 2003, **36**(2)**:** 127-139.

54. Stocking EM, Williams RM. Chemistry and biology of biosynthetic Diels-Alder reactions. *Angew Chem Int Ed* 2003, **42**(27)**:** 3078-3115.

55. Halligan KM. Synthetic and Biosynthetic Studies of the Brevianamides. PH.D thesis, Colorado State University,

2000.

56. Klas KR, Kato H, Frisvad JC, Yu F, Newmister SA, Fraley AE*, et al.* Structural and stereochemical diversity in prenylated indole alkaloids containing the bicyclo 2.2.2 diazaoctane ring system from marine and terrestrial. *Nat Prod Rep* 2018, **35**(6)**:** 532-558.

57. Li S, Finefield JM, Sunderhaus JD, McAfoos TJ, Williams RM, Sherman DH. Biochemical characterization of NotB as an FAD-dependent oxidase in the biosynthesis of notoamide indole alkaloids. *J Am Chem Soc* 2012, **134**(2)**:** 788-791.

58. Xu X, Zhang X, Nong X, Wang J, Qi S. Brevianamides and mycophenolic acid derivatives from the deep-sea-derived fungus *Penicillium brevicompactum* DFFSCS025. *Mar Drugs* 2017, **15**(2).

59. Simpson TJ, Dejesus AE, Steyn PS, Vleggaar R. Biosynthesis of aflatoxins. Incorporation of [4′-2H2]averufin into aflatoxin B1 by *Aspergillus flavus*. *J Chem Soc D* 1982(11)**:** 631-632.

60. Vleggaar R. Biosynthetic studies on some polyene mycotoxins. *Pure Appl Chem* 1986, **58**(2)**:** 239-256.

61. Marion F, Williams DE, Patrick BO, Hollander I, Mallon R, Kim SC*, et al.* Liphagal, a selective inhibitor of PI3 kinase alpha isolated from the sponge *Aka coralliphaga*: structure elucidation and biomimetic synthesis. *Org Lett* 2006, **8**(2)**:** 321-324.

62. Guo H, Benndorf R, Leichnitz D, Klassen JL, Vollmers J, Goerls H*, et al.* Isolation, biosynthesis and chemical modifications of rubterolones A-F: rare tropolone alkaloids from *Actinomadura* sp. 5-2. *Chem Eur J* 2017, **23**(39)**:** 9338-9345.

63. Hoefle G, Irschik H. Isolation and biosynthesis of aurachin P and 5-nitroresorcinol from *Stigmatella erecta*. *J Nat Prod* 2008, **71**(11)**:** 1946-1948.

64. Song Z-L, Fan C-A, Tu Y-Q. Semipinacol rearrangement in natural product synthesis. *Chem Rev* 2011, **111**(11)**:** 7523-7556.

65. Katsuyama Y, Harmrolfs K, Pistorius D, Li Y, Mueller R. A semipinacol rearrangement directed by an enzymatic system featuring dual-function FAD-dependent monooxygenase. *Angew Chem Int Ed* 2012, **51**(37)**:** 9437-9440.

66. Davison J, al Fahad A, Cai M, Song Z, Yehia SY, Lazarus CM*, et al.* Genetic, molecular, and biochemical basis of fungal tropolone biosynthesis. *Proc Natl Acad Sci U S A* 2012, **109**(20)**:** 7642-7647.

67. Godfrey RC, Green NJ, Nichol GS, Lawrence AL. Chemical synthesis of (+)-brevianamide A supports a Diels–

Alderase-free biosynthesis. *ChemRxiv Preprint* 2019.

68. Mori T, Iwabuchi T, Hoshino S, Wang H, Matsuda Y, Abe I. Molecular basis for the unusual ring reconstruction in fungal meroterpenoid biogenesis. *Nat Chem Biol* 2017, **13**(10)**:** 1066-1073.

69. Maiya S, Grundmann A, Li S-M, Turner G. The fumitremorgin gene cluster of *Aspergillus fumigatus*: identification of a gene encoding brevianamide F synthetase. *ChemBioChem* 2006, **7**(7)**:** 1062-1069.

70. Kato N, Suzuki H, Takagi H, Asami Y, Kakeya H, Uramoto M*, et al.* Identification of cytochrome P450s required for fumitremorgin biosynthesis in *Aspergillus fumigatus*. *ChemBioChem* 2009, **10**(5)**:** 920-928.

71. Matsuda Y, Iwabuchi T, Fujimoto T, Awakawa T, Nakashima Y, Mori T*, et al.* Discovery of key dioxygenases that diverged the paraherquonin and acetoxydehydroaustin pathways in *Penicillium brasilianum*. *J Am Chem Soc* 2016, **138**(38)**:** 12671-12677.

72. Quantum chemical calculations were performed using Gaussian 16, rev B.01 and Orca 4.1.2. For a full description of computational methods and references see the Supporting Information.

73. Jeon B-s, Wang S-A, Ruszczycky MW, Liu H-w. Natural [4+2]-cyclases. *Chem Rev* 2017, **117**(8)**:** 5367-5388.

74. Oikawa H. Nature's strategy for catalyzing Diels-Alder reaction. *Cell Chem Biol* 2016, **23**(4)**:** 429-430.

75. Chen M, Shao C-L, Fu X-M, Xu R-F, Zheng J-J, Zhao D-L*, et al.* Bioactive indole alkaloids and phenyl ether derivatives from a marine-derived *Aspergillus* sp fungus. *J Nat Prod* 2013, **76**(4)**:** 547-553.

76. Zhu M, Zhang X, Feng H, Dai J, Li J, Che Q*, et al.* Penicisulfuranols A-F, alkaloids from the mangrove endophytic fungus *Penicillium janthinellum* HDN13-309. *J Nat Prod* 2017, **80**(1)**:** 71-75.